Development of a PIXE method at high energy with the ARRONAX cyclotron

D. Ragheb · C. Koumeir · V. Métivier ·
J. Gaudillot · A. Guertin · F. Haddad ·
N. Michel · N. Servagent

Abstract The high energy PIXE (HEPIXE) method is a multi-elemental non-destructive ion beam analysis technique. It is based on the detection of the X-ray emitted due to the interaction of high energy particle beam with a sample. This technique is fast and allows the analysis of heavy and medium elements in thin (μm), thick (mm) and multilayer samples. At the ARRONAX facility (Nantes, France), the HEPIXE method has been used to determine the composition of natural and synthetic sodalites. Photochromic properties of these samples are supposed to come from the trace elements (concentration in the ppm range) present in the samples. Taking advantage of the 70 MeV proton beam available at our facility, the HEPIXE method has been also used to study multilayer samples. It has been shown that it is possible to determine the composition of each layer, their thicknesses and their depth position by analyzing the recorded X-ray spectra.

Keywords High energy PIXE · Ion beam analysis · Non-destructive analysis · Multilayer · ARRONAX

Introduction

PIXE, Particle Induced X-ray emission, is a well-established method for non-destructive elemental concentration determination [1]. It is mainly used with protons of incident energy below 4 MeV and has been applied in many different fields from aerosols characterization, biology, geology, art and archeology [2–4]. The PIXE method is based on the detection of the X-rays produced during the electron rearrangement following the interaction between the incoming particle and the target atoms. Usually, the K X-ray lines are detected for the lighter elements ($Z < 50$) whereas L X-ray lines are used for heavier elements due to small production cross sections for K X-rays [5, 6]. This analysis method, which uses low energy projectile, provides a valuable tool for thin layers analysis (a few tens of micrometers). For the analysis of thick samples, higher beam energy is required. With a High Energy PIXE (HEPIXE) method, the projectile penetrates deeper inside the sample and favors the production of K X-ray lines which are more energetic than L X-ray lines and are less attenuated in matter. This is particularly interesting for heavy elements [7].

However, the high-energy PIXE method needs accelerators more expensive and less available than the usual PIXE technique. The ARRONAX cyclotron, commissioned in 2010, is a new and unique experimental facility delivering protons from 30 up to 70 MeV, deuterons from 15 up to 35 MeV and alpha particles at fixed 68 MeV [8]. It is dedicated both to the production of innovative radionuclide for medical applications and to studies of radiation interaction with inert and living matter. The HEPIXE method is part of its scientific program. The HEPIXE method presents several advantages: thick targets can be studied thanks to the large range of the energetic beam and to the small absorption of the K X-rays for medium and heavy element; data analysis is quite simple due to the slow evolution of the X-ray emission cross sections [9] and the small overlapping of related lines. The samples can be

D. Ragheb · C. Koumeir · V. Métivier (✉) · J. Gaudillot ·
A. Guertin · F. Haddad · N. Michel · N. Servagent
SUBATECH, IN2P3-CNRS, Ecole des Mines de Nantes,
Université de Nantes, 4 Rue Alfred Kastler, 44307 Nantes,
France
e-mail: vincent.metivier@subatech.in2p3.fr

C. Koumeir · J. Gaudillot · F. Haddad · N. Michel
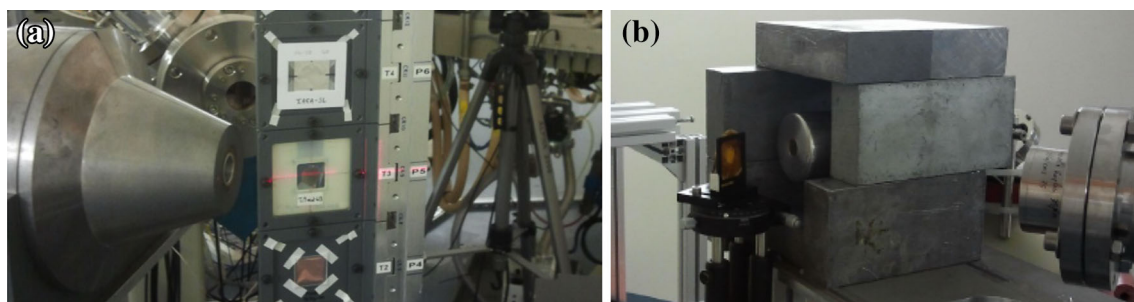GIP ARRONAX, 1 Rue Aronnax, 44817 Saint Herblain, France

Fig. 1 The HE-PIXE experimental set-up, the beam line extraction window, the target display and the LEGe detector inside two shielding configurations: **a** a three layer (Pb/Cu/Al) bulky one (on the *left*); **b** a more compact one with single lead bricks (on the *right*)

analyzed in normal air which is essential especially for art or cultural heritage objects [9–12].

The paper is organized as follow. The experimental setup and analysis method are presented first; then, two applications performed at our facility are described. The first one fits in the scope of elemental trace analysis whereas the second one is connected to multilayer analysis. Finally, some perspectives are proposed to complete and improve this method.

Materials and methods

Experimental set-up

The experimental setup for the HEPIXE analysis method at ARRONAX can be seen in Fig. 1. The experiment is performed in normal air after the release of the charged particle beam through a 75 μm Kapton window. X-rays emitted due to the interaction of the high energy particle beam with the sample are collected by a high purity low energy germanium detector LEGe from Canberra [13] cooled to the LN_2 temperature. The angle of detection is chosen to be 135° with respect to the beam line, to limit the effects of secondary electron bremsstrahlung [14]. The beam intensity is measured using a Faraday cup (that acts as a beam stop, located 30 cm behind the target) and/or a thin monitor foil when the target thickness is too large or the incoming particle energy too low to collect reliable measurement with the Faraday cup. The monitor foils used are 2 μm copper: the number of collected K X-rays is directly related to the beam intensity. Beforehand, a calibration of this measurement is made with the faraday cup (without other target).

To reduce the dead time of the detector and data acquisition system and to reduce the background level, beams are delivered at low intensities (of the order of 1 nA or less) and the detector is shielded using a three layer assembly (5 cm lead, 2 cm copper and 2 mm aluminum) (Fig. 1 left). This layered composition removes

characteristic X-rays of Cu and Pb, but it does not allow the detector to be closer than 16 cm from the target. A simple 5 cm lead brick shielding is used when it is necessary to reduce this distance (down to 6 cm) (Fig. 1 right).

X-ray spectrum is digitalized using a multichannel analyzer and the acquisition is made with the Genie 2000 software from Canberra. The detector and the acquisition unit are calibrated in energy and efficiency with standard radioactive sources (CERCA LEA).

Elemental concentration determination

The analysis of the peaks contained in the collected X-ray spectrum allows identifying and quantifying the elements present in the sample thanks to their characteristic K lines. For each element, the detection limit [5] depends on the detection efficiency, the X-ray absorption in the air and in the sample (self-absorption), the production cross section of X-rays (K-lines) and the background level (from bremsstrahlung and Compton diffusion) [15] coming from the interaction of particles with the sample, the beam line and the beam stop.

Once the elements are identified, we can assay their concentrations. The number of photons detected by unit time from the element of atomic number Z is determined using formula (1) [5]:

$$N_i = N_P C_i \omega_{K_i} b_{ij} T_{abs_i} \varepsilon_i \frac{\Omega}{4\pi} \int_{E_0}^{E_{min}} \frac{\sigma_i(E) T_{target}(E)}{S(E)} dE \qquad (1)$$

with N_P, the number of particles per unit time from an uniform beam with a section lower than the sample diameter; C_i, the concentration of the element i per unit volume; σ_i, the effective ionization cross section of the electronic layer of the element i [16]; ω_{Ki}, the fluorescence yield of the element i for a specific transition; b_{ij}, the relative intensity for a considered X-ray for the element i [17, 18]; T_{target}, the total attenuation within the target and T_{abs_i} the total attenuation in the whole medium between the output of the sample and the detector entrance (any filter,

Table 1 Characteristics of the target samples

Sample	Natural sodalite	Synthetic sodalite	IAEA RM SL-1
Origin	IMN	IMN	IAEA
Form	Pellet	Pellet	Pellet
Mass	216.9 mg	94.2 mg	400 mg
Thickness	1200.74 μm	521.74 μm	552 μm
Diameter	1 cm	1 cm	2.2 cm
Density	2.3	2.3	2.1

air, entrance windows, etc.); ε_i, the detector efficiency for K X-rays related to the element i [19]; Ω, the solid angle of detection; $S(E)$, the stopping power of the target, E_0 and E_{min} corresponding to, respectively, the incoming particle energy and the output particle energy. The number of photon in a given peak in spectra is determined using the Fitzpeak software [20], completed with a homemade fitting code for some overlapping peaks.

In a thick target, the X-ray production cross section varies with the energy of the particle throughout its path in the sample; moreover, the K X-ray's self-attenuation depends on the target's matrix. So, the resolution of this equation involves knowing the composition of the matrix and the change of beam's energy throughout the sample. Depending on the precise knowledge of the whole factors from the Eq. (1) or not, this equation can be used directly to determine the concentration of the elements, or indirectly by use of a reference sample method, an internal standard's method or standard addition's method [5].

Two types of sodalite [21], a natural mineral one and a synthetic product, was provided by the "Institut des Matériaux Jean Rouxel" in Nantes (IMN) in order to be analyzed by the HEPIXE technique at ARRONAX. The idea is to compare, in composition and amount, natural and synthetic sodalite in order to compare the two samples and investigate the mechanism of the photochromic effect [22].

For this purpose, we choose to perform the analysis using a standard sample as reference to increase the accuracy of the method, minimizing the possible bias related to cross section estimation, energy loss calculation, detector efficiency and incident particle flux measurements. The matrix of the reference sample, in terms of density and composition, has to be as close as possible to that of the samples and has to be analyzed under the same experimental conditions. Hence, we use the reference material IAEA RM SL-1 (lake sediment), provided with a certificate detailing the trace and minor elements present and their concentrations in ppm (mg kg^{-1}) [23]. The characteristics of the 3 samples are presented in the Table 1. The natural sodalite stone was ground and pelletized so that it has the same characteristics as the other samples.

In order to correct the self-absorption of K X-rays in the sample and to estimate the variation of the beam's energy, one has to know the major components of the matrix. To do this, we have used Scanning Electron Microscopy (SEM) coupled with energy dispersive microanalysis X-ray (EDX) at the IMN. Because of lack of material, we were not able to determine the matrix of synthetic sodalite. We have assumed that this matrix was close to natural sodalite and have corrected the self-absorption in this sample the same way.

The elemental concentration determination for the three samples was performed with a 68 MeV alpha particle beam, in order to maximize the K X-ray emission in a wide range of elements. The effective energy of the alpha particles impinging the target is 62.8 ± 0.2 MeV after their crossing of the Kapton window and the air between this window and the target (SRIM calculation [24]). Beam intensity was around 100 pC and irradiation time a few hundred of seconds. Targets were located at 25 cm away from the beam extracting window and the detector at 7.5 cm from the target, at an angle of 135° with the beam direction.

Multilayer analysis

Taking full advantage of the high penetration of protons or light ions at around 70 MeV allows us not only to extract information on the elemental composition of materials, but also on the distribution in the depth of the present elements. The first foreseen application concerns multilayer samples for which one wants to determine the elemental nature of each layer, their thickness and their position in depth. Those informations are extracted by taking account of the difference of K X-ray absorption for the different elements and for different K X-ray lines of a single element. The method proposed here doesn't need the detection of additional gamma rays as published previously [25].

For a given multilayer target, the layer sequence can be determined thanks to the ratio of the intensities of the detected K_α and K_β lines (K_α/K_β) [26, 27]. The layer thickness can be determined thanks to the attenuation of a single line (mostly the K_α one).

The K_α line intensity and the ratio of K_α/K_β lines intensities of a layer are explicitly given by the Eqs. (2) and (3) respectively:

$$I_{K_\alpha}^i = N_p C_i \sigma_K b_\alpha^i \varepsilon_\alpha^i \int_0^{d_i} \exp(-\mu_\alpha^i y)dy \sum_{j=1}^{i-1} \exp(-\mu_\alpha^j d_j) \quad (2)$$

$$\frac{I_{K_\alpha}^i}{I_{K_\beta}^i} = \frac{\mu_\alpha^i}{\mu_\beta^i} \frac{b_\alpha^i}{b_\beta^i} \frac{\varepsilon_\alpha^i}{\varepsilon_\beta^i} \frac{\int_0^{d_i} \exp(-\mu_\alpha^i y)dy}{\int_0^{d_i} \exp(-\mu_\beta^i y)dy} \sum_{j=1}^{i-1} \frac{\exp(-\mu_\alpha^j d_j)}{\exp(-\mu_\beta^j d_j)} \quad (3)$$

where $\mu_{\alpha,\beta}$ represents the absorption coefficient, $b_{\alpha,\beta}$ the natural intensity ratio of α,β lines, σ_K the K X-ray production cross section and dj the thickness of each layer. In these equations, it is assumed that the target thickness is at maximum of the order of several hundreds of micron, so that the cross section remains practically constant considering the energy loss of high energy protons (70 MeV) negligible.

Once the element constituting the layers identified by their characteristic X-rays in the spectrum, the thicknesses are calculated [thanks to the Eq. (2)] assuming each layer is in the first position. Those thicknesses are called apparent thicknesses. Then, the K_α/K_β ratios are calculated for each element according to these values. The element that present a calculated ratio (K_α/K_β) equal or close to the experimental ratio is considered to be in the first position. Then, new apparent thicknesses for the remaining elements are computed, taking into account the effect of K_α's absorption in the first layer. Similarly, we compare the new calculated and experimental ratios (K_α/K_β) to determine which layer is in second position, and so on. This iterative process allows estimating the thickness of the various layers and their position in depth.

This method will be illustrated in the Sect. 3.2 with is a sample constituted of three layers, respectively Ti, Ag, Au. The particle beam consists of protons at 70 MeV and the detector is located at an angle of 135° relative to the beam direction and 26 cm from the target. Reference foils are used to normalize the K X-ray intensity for each element in order to eliminate the influence of both detection efficiency and ionization cross sections, not necessarily well known. The reference foils are high purity standard materials (from Goodfellow) and have thicknesses about 10 μm. These thicknesses are precisely measured: each layer foil is weighed separately before irradiation using an accurate scale ($\pm 10^{-8}$ kg) and its area is evaluated thanks to a calibrated desktop scanner. Knowing the density of each material and assuming the thickness to be homogeneous over the whole surface, the thicknesses have been deduced (Ti: 9.95 μm; Ag: 10.34 μm; Au 10.75 μm) accurately. For such thicknesses, the change in the ionization cross section with protons at 70 MeV can be neglected. The beam intensity is around of 100 pA and the irradiation time is about few minutes. Each K line intensity is normalized to the number of incident particle measured by a monitor sheet (2 μm copper) set on front of the sample.

Results

Elemental trace analysis in sodalite samples

Both natural and synthetic sodalite samples are irradiated with a 68 MeV alpha particle beam (62.8 MeV at the entrance of the sample, see Sect. 2.2). The Fig. 2 represents the collected K X-ray spectrum for the synthetic sample. The abscissa axis stands for the energy of detected X-rays and the ordinate axis (in logarithm scale) the number of counts. Characteristic X-ray lines are superimposed on a continuous background. Elements from which these lines are emitted are identified on the spectrum. The Argon contribution is due to the interaction of the beam with the air.

The concentrations of identified elements are presented in Table 2 for synthetic sodalite and in Table 3 for natural sodalite. These concentrations in the sodalite samples have been determined by normalizing each X-ray peak in the spectrum with the one which has the closest energy in the reference sample (relative method). Uncertainties are calculated from the statistical uncertainties on the number of counts in the X-ray lines related to the considered elements in the analyzed and reference samples, combined with uncertainties associated to the recommended values of the elemental concentration in the reference sample [23] and with the uncertainties on thicknesses of the samples. These uncertainties are generally in the range from 10 to 20 %, and can go up to 30 % and more when the statistics in the peak is poor. These uncertainties are mainly related both to the recommended values and to the peak statistics. Possible improvement is possible when increasing the irradiation time, but with limitation due to uncertainties on the recommended values.

For element lighter than calcium (Z = 20), X-ray energies are too low to be detected and quantified because of the absorption in the air between the sample and the detector. We are nonetheless able to identify chlorine, but its quantification is imprecise due to the low proportion of X-rays reaching the detector combined to the close large peak related to argon.

Regarding the qualitative analysis, one can note that different elements are present in the two samples of sodalite: chlorine and tin are detected only in the synthetic product, while gallium, bromine, silver and iodine are only found in the natural sample. Regarding the elements detected in both samples, they are not present in the same quantity. These first results show that the HEPIXE technique has put in evidence differences in the composition between natural and synthetic sodalite which can give hints about their different properties. This will help to understand their photochromic properties and perform new synthesis method. However, elements with lower atomic number than calcium could not be detected here, as well as those present in quantity lesser than the limit of detection.

With the present experimental configuration, the limit of detection of this HEPIXE technique is of the order of several tens of ppm for elements heavier than calcium. If one needs to lower this limit of detection, one have mainly to minimize the absorption of X-rays in the air, by reducing
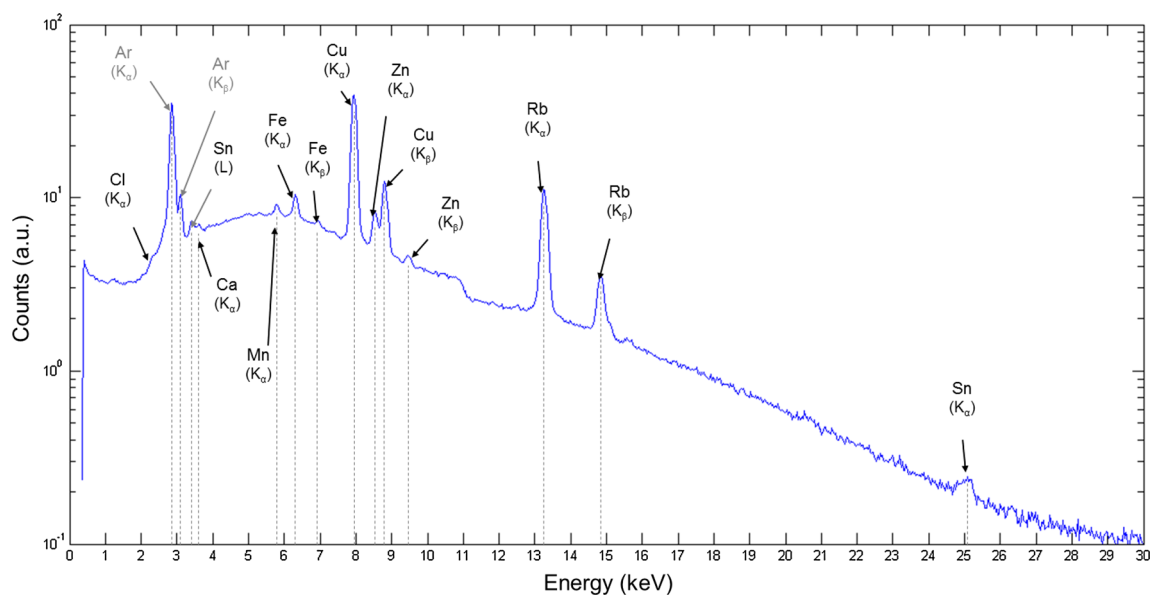
Fig. 2 Energy spectrum of the detected X-rays for the synthetic sodalite sample irradiated by alpha particles at 68 MeV

Table 2 Concentrations with associated uncertainties of the elements detected in the synthetic sodalite

Element	X-ray	Energy (keV)	Concentration (mg kg^{-1})	Uncertainty (mg kg^{-1})
Ca	K_α	3.7	4,655	±1,303
Mn	K_α	5.9	667	±113
Fe	K_α	6.4	943	±132
Cu	K_α	8.0	1,709	±290
Zn	K_α	8.6	492	±83
Rb	K_α	13.3	766	±137
Sn	K_α	25.2	53	±14

Table 3 Concentrations with associated uncertainties of the elements detected in the natural sodalite

Element	X-ray	Energy (keV)	Concentration (mg kg^{-1})	Uncertainty (mg kg^{-1})
Ca	K_α	3.7	9,193	±1747
Mn	K_α	5.9	373	±104
Fe	K_α	6.4	8,128	±1,138
Cu	K_α	8.0	3,498	±514
Zn	K_α	8.6	247	±44
Ga	K_α	9.2	18	±5
Br	K_α	11.9	123	±20
Rb	K_α	13.3	93	±16
Ag	K_α	22.1	39	±15
I	K_α	28.6	97	±25

the distance between the sensor and the sample or by placing them in the vacuum, if necessary and/or achievable.

Table 4 Apparent thicknesses and K_α/K_β ratio calculated with the iterative multilayer procedure

	Layer	Apparent thickness (µm)	Calculated K_α/K_β	Experimental K_α/K_β
Step 1	**Ti**	61.5	3.6	3.5
	Ag	24.4	4.4	3.06
	Au	7.5	1.003	0.69
Step 2	(Ti) **Ag**	48.3	3.6	3.06
	(Ti) **Au**	7.7	0.998	0.69
Step 3	(Ti) **Ag**	131.0	3.06	3.06
Step 4	(Ti Ag) **Au**	10.5	0.67	0.69

Multilayer analysis

A multilayer sample is analyzed thanks to the HEPIXE method. These measurements are made blindly, even if we know exactly the thickness of the layers used in the sandwich. These thicknesses were initially measured with the same procedure as for the reference foils (from precise weight and area measurements). These values are reported in Table 5 and referred as real thicknesses. Associated uncertainties are calculated by propagating the uncertainties in measurements of the various involved quantities. The iterative procedure described in Sect. 2.3 is then applied, analyzing the collected X-ray spectrum when a 70 MeV proton beam irradiates the multilayer sample. With this sample, four steps are needed and are reported in the Table 4.

First, three elements (Ti, Ag, Au) are identified and "apparent" thicknesses are calculated (step 1); one can

Table 5 Thicknesses in a multilayer sample evaluated thanks to the HEPIXE method

Element	Evaluated thickness (μm)	Real thickness (μm)
Ti	131.0 ± 2.3	129.1 ± 1.3
Ag	48.3 ± 1.5	49.4 ± 0.5
Au	10.5 ± 0.4	10.4 ± 0.1

conclude that titanium is in the first layer, but the discrepancy in the K_α/K_β ratios indicates that its thickness is underestimated (due to complete attenuation of deeper K_α X-rays in the titanium foil). Nevertheless, new apparent thicknesses for the silver and gold foils are calculated considering the titanium foil before (step 2), but obviously no K_α/K_β ratios agree; the thickness of the titanium foil is then reevaluated considering the attenuation of the K_α X-rays from the silver (step 3), leading to coherent values for the K_α/K_β ratios. Finally, we have only to calculate the thickness of the gold foil behind the titanium and the silver foils (step 4). The results are reported in the Table 5 and can be compared to the "real" thicknesses; a very good agreement between the results given by the HEPIXE method and the characteristics of the multilayer sample both for the composition, thickness and layer sequence is found.

This result allows us to highlight the ability of the HE PIXE method to determine multilayer sample composition, including the measurement of the thickness of the various layers. As the production cross section of KX-ray evolves slowly with high energy protons, normalization with standard material is facilitated and precise analysis of the target achieved. This is done using the single information delivered by X-rays. However, adding detection of the gamma rays emitted during the interaction of the beam with the target [25], additional information would be available to solve more complex multilayer configuration, for example when several layers of the same composition are present in the sample.

Conclusion and perspectives

The high energy PIXE method allows performing elemental concentration determination for medium and heavy elements in thin (μm) and thick (mm) samples. It's under development at the ARRONAX cyclotron as a fast, in air, non-destructive, ion beam multi-elemental analysis technique. Elemental concentration determination for element heavier than potassium in matrix such as sodalite has been demonstrated, at the ppm level, using standard material as reference. In order to achieve the detection and the

quantification of lighter elements, the set-up will be completed with a smaller silicon drift detector (which can be located closer to the target for higher efficiency and less absorption in air for low energy X-rays) and with a germanium detector for gamma rays detection (combined HEPIXE/PIGE). Thick multilayer analysis has also been demonstrated, achieving notably the detection of elemental composition, thickness and position in depth of a specially designed assembly of Ti (130 μm), Ag (50 μm) and Au (10 μm). This technique will be applied to industrial multilayer material, cultural heritage objects, corroded objects, etc.

References

1. Johansson SAE, Johansson TB (1976) Nucl Instrum Methods 137:473–516
2. Caijin X, Guiying Z, Donghui H, Bangfa N, Cunxiong L, Yali Q, Hongchao S, Pingsheng W, Weizhi T (2012) J Radioanal Nucl Chem 291:95–100
3. Sarita P, Naga Raju GJ, Pradeep AS, Rautray TR, Reddy BS, Reddy SB, Vijayan V (2012) J Radioanal Nucl Chem 294:355–361
4. Lesigyarski D, Šmit Z, Zlateva-Rangelova B, Koseva K, Kuleff I (2013) J Radioanal Nucl Chem 295:1605–1619
5. Johansson SAE, Campbell JL, Malmqvist KG (1995) Particle-induced X-ray emission spectrometry (PIXE). Chem Anal 133:33–35
6. Romo-Kröger CM (2010) Vacuum 84:1250–1253
7. Denker A, Bohne W, Campbel JL, Heide P, Hopman T, Maxwell JA, Opitz-Coutureau J, Rauschenberg J, Röhrich J, Strub E (2005) X-Ray Spectrom 34:376–380
8. Haddad F, Michel N, Guertin A, Barbet J, Chatal J F, Martino J (2007) In: Proceedings of the international conference on nuclear data for science and technology, Nice, France, pp 1383–1385
9. Denker A, Maier KH (1999) Nucl Instrum Methods Phys Res B 150:118–123
10. Dran JC, Salomon J, Calligaro T, Walter P (2004) Nucl Instrum Methods Phys Res B 219–220:7–15
11. Dupuis T, Chêne G, Mathis F, Marchal A, Philippe M, Garnir HP, Stirvay D (2010) Nucl Instrum Methods Phys Res B 268:1911–1915
12. Won-in K, Suksawang S, Thongleurm C, Intarasiri S, Tippawan U, Kamwanna T, Dararutana P (2012) J Radioanal Nucl Chem 294:383–386
13. http://www.canberra.com/products/detectors/germanium-detectors.asp
14. Ishii K (2006) Radiat Phys Chem 75:1135–1163
15. Koumeir C, Haddad F, Métivier V, Servagent N, Michel N (2011) In: Proceeding of European conference on X-ray spectrometry,

20–25 June 2010, Figueira da Foz, Coimbra, Portugal, 23–33. arXiv:1011.4057v1 [nucl-ex]

16. Cipolla SJ (2007) Nucl Instrum Methods Phys Res B 261:142–144
17. Salem SI, Panossian SL, Krause RA (1974) Atomic Data Nucl Data Tables 14:91–109
18. Krause MO (1979) J Phys Chem Ref Data 8:307–327
19. Mohanty BP, Balouria P, Garg ML, Nandi TK, Mittal VK, Govil IM (2008) Nucl Instrum Methods Phys Res A 584:186–190
20. FitzPeaks Gamma Analysis and Calibration Software version 3.66, based on methods presented. In: Koskelo MJ, Aarnio PA, Routti JT (1981) Nucl Instr Meth 190:89–99
21. Medved DB (1954) Am Mineral 39:615–629
22. Pizani PS, Terrile MC, Farach HA, Poole C Jr (1985) Am Mineral 70:1186–1192
23. http://nucleus.iaea.org/rpst/Documents/rs_iaea-sl-1.pdf
24. Ziegler JF, Ziegler MD, Biersack JP (2010) Nucl Instrum Methods Phys Res B 268:1818–1823
25. Koumeir C, Haddad F, Métivier V, Servagent N, de la Bernardie X, Garrido E, Ragheb D (2011) Applications of nuclear techniques. AIP Conf Proc 1412:105–112
26. Demortier G, Mathot S, Oystaeyen VB (1990) Nucl Instrum Methods Phys Res B 49:46–51
27. Demortier G, Mathot S, Steukers C (1993) Nucl Instrum Methods Phys Res B 75:347–354